WAGENINGEN
UNIVERSITY & RESEARCH

Uncertainty quantification of nitrogen use efficiency prediction in China using Monte Carlo simulation and quantile regression forests

Computers and Electronics in Agriculture

Liu, Yingxia; Heuvelink, Gerard B.M.; Bai, Zhanguo; He, Ping

https://doi.org/10.1016/j.compag.2022.107533

This publication is made publicly available in the institutional repository of Wageningen University and Research, under the terms of article 25fa of the Dutch Copyright Act, also known as the Amendment Taverne.

Article 25fa states that the author of a short scientific work funded either wholly or partially by Dutch public funds is entitled to make that work publicly available for no consideration following a reasonable period of time after the work was first published, provided that clear reference is made to the source of the first publication of the work.

This publication is distributed using the principles as determined in the Association of Universities in the Netherlands (VSNU) 'Article 25fa implementation' project. According to these principles research outputs of researchers employed by Dutch Universities that comply with the legal requirements of Article 25fa of the Dutch Copyright Act are distributed online and free of cost or other barriers in institutional repositories. Research outputs are distributed six months after their first online publication in the original published version and with proper attribution to the source of the original publication.

You are permitted to download and use the publication for personal purposes. All rights remain with the author(s) and / or copyright owner(s) of this work. Any use of the publication or parts of it other than authorised under article 25fa of the Dutch Copyright act is prohibited. Wageningen University & Research and the author(s) of this publication shall not be held responsible or liable for any damages resulting from your (re)use of this publication.

For questions regarding the public availability of this publication please contact
openaccess.library@wur.nl

Computers and Electronics in Agriculture 204 (2023) 107533

Contents lists available at ScienceDirect

Computers and Electronics in Agriculture

journal homepage: www.elsevier.com/locate/compag

Uncertainty quantification of nitrogen use efficiency prediction in China using Monte Carlo simulation and quantile regression forests

Yingxia Liu [a,b,c], Gerard B.M. Heuvelink [b,c], Zhanguo Bai [c], Ping He [a,*]

[a] Key Laboratory of Plant Nutrition and Fertilizer, Ministry of Agriculture and Rural Affairs/Institute of Agricultural Resources and Regional Planning, Chinese Academy of Agricultural Sciences, Beijing 100081, PR China
[b] Soil Geography and Landscape group, Wageningen University, P.O. Box 47, 6700 AA Wageningen, the Netherlands
[c] ISRIC – World Soil Information, P.O. Box 353, 6700 AJ Wageningen, the Netherlands

ARTICLE INFO

Keywords:
Nitrogen use efficiency
Input data
Model uncertainty
Monte Carlo
Quantile regression forests

ABSTRACT

Nitrogen use efficiency (NUE) plays an essential role in food security and environmental sustainability. With the development of technology, NUE prediction by models has come available. However, the prediction uncertainty of NUE models is still poorly understood. This study aimed to analyze uncertainty in NUE predictions obtained from a random forest machine learning model. Input and model uncertainties were quantified using Monte Carlo simulation in three scenarios and quantile regression forests (QRF), respectively, to analyze how these uncertainties propagate to the NUE predictions for 31 provinces in China from 1978 to 2015. Two NUE indicators were considered: the partial factor productivity of nitrogen (PFP_N) and the partial nutrient balance of nitrogen (PNB_N). The results indicated that the prediction uncertainty for both NUE indicators decreased over time. In 2015, PFP_N had a higher 90% prediction interval ratio (PIR_{90}) of input data in south and west China and a higher 90% prediction interval width (PIW_{90}) in south and east-coastal China, while PNB_N had a higher PIR_{90} in north China and a higher PIW_{90} in northeast China. The NUE prediction uncertainty propagated from QRF models had similar spatial patterns as those resulting from uncertainty in input data. NUE in most provinces had smaller input uncertainty than model uncertainty, except PNB_N, which had smaller model uncertainty than input uncertainty after 2010. Generally, PNB_N had higher input uncertainty contributions than PFP_N in 2015, especially in south and northeast China. Overall, the uncertainties in NUE predictions were substantial. A series of recommendations were made to improve the accuracy of NUE predictions. These may be applied by the government, in order to inform sustainable nitrogen management in agroecological systems.

1. Introduction

The Sustainable Development Goals defined by the United Nations call to action to ensure agricultural and environmental sustainability. Nitrogen (N) is one of the most important nutrients for crop growth, contributing more than 50 % of the crop yield increase (Stewart et al., 2005; Zhang et al., 2015; Dimkpa et al., 2020). Studies demonstrated that excessive N application causes diminishing returns for increased crop yields and N removals, especially in China (Zhang et al., 2015). In other words, excessive N application leads to decreased nitrogen use efficiency (NUE). NUE indicators are major detection instruments related to food security, environmental pollution, economic development and resource use, and are widely and increasingly used by agronomists, environmental scientists, biogeochemists, policymakers and other stakeholders at various temporal and spatial scales (Quan et al., 2021). The partial factor productivity of N (PFP_N, in kilograms of grain per kilogram of N applied) and partial nutrient balance of N (PNB_N, in kilograms of N removal by aboveground crop per kilogram of N applied) are two popular indicators to reflect NUE averages and trends (Dobermann, 2007). Specifically, NUE in China (38 and 0.40 kg kg^{-1} yr^{-1} for PFP_N and PNB_N, respectively) (Liu et al., 2020b) is much lower than in well managed systems in other parts of the world (greater than 60 and 0.70–0.90 kg kg^{-1} yr^{-1} for PFP_N and PNB_N, respectively) (Roberts, 2007; Fixen et al., 2015). Therefore, improving NUE indicators to a reasonable range is vital to environmental sustainability in China.

Many studies revealed that NUE has large spatial and temporal variations as a consequence of different crops, climate, soil properties and management practices (Zhang et al., 2015; Liu et al., 2020a). For

* Corresponding author.
E-mail address: heping02@caas.cn (P. He).

https://doi.org/10.1016/j.compag.2022.107533
Received 22 June 2022; Received in revised form 16 November 2022; Accepted 25 November 2022
Available online 9 December 2022
0168-1699/© 2022 Elsevier B.V. All rights reserved.

example, PFP_N changed from 86, 56 and 74 kg kg^{-1} in 1960 to 26, 30 and 69 kg kg^{-1} in 2009 in China, India and USA, respectively (Lassaletta et al., 2014). Statistical modelling can support the understanding of the causes of the spatial and temporal variations (Li et al., 2020; Liu et al., 2020b; Zhang et al., 2021b). Random forest (RF), as one of the machine learning algorithms, stands out due to its flexibility and competitive explanatory performance. A disadvantage of RF is that the model cannot be presented as a limited set of equations, which makes it difficult to interpret (Robinson et al., 2017). Li et al. (2020) used RF and found that mean annual temperature was the most critical factor of PFP_N improvement. Ren et al. (2019) applied RF to analyze the effects of manure on recovery efficiency of N, and found that soil properties contributed up to 55 %, followed by climatic factors that contributed 32 %. N application rate and crop types only contributed 8.3 % and 4.6 %, respectively. Correndo et al. (2021) explored the driving factors of maize yield without N fertilizer using RF, and found that previous crop, irrigation and soil organic matter were the most relevant factors.

Even though the explanatory performance of RF models is often high compared to other models, no model is perfect and model predictions have errors, which might influence their explanatory ability. Models are useful tools to support increasing policy interest in monitoring and reporting performance of sustainable agriculture and sustainable nutrient management practices, but only if their accuracy is sufficient. So far, current research rarely addressed prediction uncertainty of NUE models, even though this restricts their application. Additionally, the sources of uncertainty and their contribution to the model output uncertainty are as yet poorly understood. Generally speaking, the main uncertainty sources originate from model inputs, model parameters and model structure (Heuvelink et al., 1989; Kay et al., 2009). Consequently, all three will propagate to the model output.

The uncertainty of model inputs includes uncertainties in measurements, such as yield and fertilizer inputs, and uncertainties in calculation parameters, such as straw return and manure coefficients. When collecting data, measurement uncertainty can be caused by many factors, such as sampling error, human error, instrument error, and parameter error in data processing (e.g., N content in manure, straw and grain ratio). These uncertainties propagate to the model output (i.e., NUE predictions). Zhang et al. (2021b) discussed the uncertainty sources of the N budget, such as calibration parameters, data sources and calculation methods. A popular method to calculate the uncertainty is Monte Carlo simulation, as: 1) it can yield the full output probability distribution, not only the variance; 2) approximation errors can be made arbitrarily small; 3) it works with any model and is easy to implement. However, an important disadvantage of the Monte Carlo method is that it is computationally demanding (Knape and Valpine, 2016). Zheng et al. (2012) applied Monte Carlo simulation to identify key uncertainty sources of atmospheric ammonia emission by simulating input data based on the reliability and accuracy of data sources, estimation methods used, and uncertainty in emission factors and by propagating uncertainties in model inputs through source-based emission models. Miller et al. (2020) used the Monte Carlo method to propagate the uncertainty of N application measurements to the overall N application rate. Kros et al. (2012) also used the Monte Carlo method to quantify the propagation of input uncertainty from initial values, model parameters, and environmental constants and variables to model outputs (N fluxes). Although computationally demanding, the Monte Carlo has shown to be an effective method for quantifying the propagation of input and parameter uncertainties to model outputs.

In addition to uncertainty in model input, there is also uncertainty caused by the model itself, because even if the inputs are error-free, the output is still imperfect. This is because a model is only a simplified representation of reality (Heuvelink, 1998b). De Vries et al. (2011) estimated the model structural uncertainty for N budgets for European agriculture by using an ensemble of modelling approaches. In machine learning, quantile regression forests (QRF) were developed and used to assess the uncertainty associated with model-derived predictions (Meinshausen, 2006; Córdoba et al., 2021). Lalitha et al. (2021) used QRF to quantify the model uncertainty of soil depth prediction, while Vaysse and Lagacherie (2017) showed that QRF provided more accurate and interpretable predicted patterns of uncertainty than regression kriging in operational digital soil mapping.

The aim of this paper is to quantify the uncertainty and uncertainty source contributions in random forest predictions of NUE using a Monte Carlo analysis and QRF for 31 provinces in China for the years 1978 to 2015. Specifically, the objectives of this paper are to: 1) use expert judgement and scenarios to quantify the uncertainty (by probability distributions) in calculations of PFP_N and PNB_N (through propagating uncertainty in crop yield, N removal, and N input); 2) analyze how uncertainty in inputs propagates through the RF model using a Monte Carlo uncertainty propagation analysis; 3) analyze how model uncertainty leads to uncertainty in model outputs using QRF; and 4) compare the contributions of input uncertainty and model uncertainty to the overall model output uncertainty. To facilitate the robustness of the results, three scenarios were defined for input uncertainty quantification, i.e., optimistic, reference and pessimistic. One of these input uncertainty scenarios (i.e., the reference scenario) was compared with model uncertainty. The results of this study can be used to benchmark new national food security projections and quantitative scenario studies and inform policy analysis and the public debate on improved data collection and model building.

2. Materials and methods

2.1. Study area and NUE indicators

The study area is defined by 31 provinces of China (excluding Hong Kong, Macao and Taiwan), for a time period from 1978 to 2015. The target variables studied were two indicators for long-term trends of NUE: PFP_N and PNB_N (Table A1) (Dobermann and Cassman, 2005; Dobermann, 2007). The indicators were calculated using the data from the National Bureau of Statistics of China in 2019 (https://data.stats.gov.cn). The data includes economic yield of different crops, human and livestock numbers, chemical fertilizer and related parameters, as listed in Table A1. More details are given in He et al. (2018). The key steps of the uncertainty analysis are shown in Fig. 1.

2.2. Uncertainty of input data

2.2.1. Measurement errors represented by probability distributions

This study used official data which should be trustworthy. However, no measurement is error-free, among others due to the use of different equipments in field and lab and over time, and sampling errors. In addition, the uncertainty of the input parameters used to calculate N removal and N input can be different between provinces and over different years. Measurement errors can also be correlated in space and time, because similar biases can be made in subsequent years or in neighboring provinces.

Measurement error can be mathematically represented as follows:

$$Y_t = Y_m + \varepsilon \quad (1)$$

where Y_t and Y_m are the true and measured values of an input variable, respectively; and ε is a measurement error (i.e., the difference between the true and measured value).

The actual measurement errors are unknown and therefore represented by probability distributions. A major task is then to quantify the statistical parameters of these probability distributions. The following assumptions were made to be able to do this for yield, N removal and N input:

- All measurement errors were assumed to be normally distributed. This substantially facilitates the subsequent statistical analysis and is

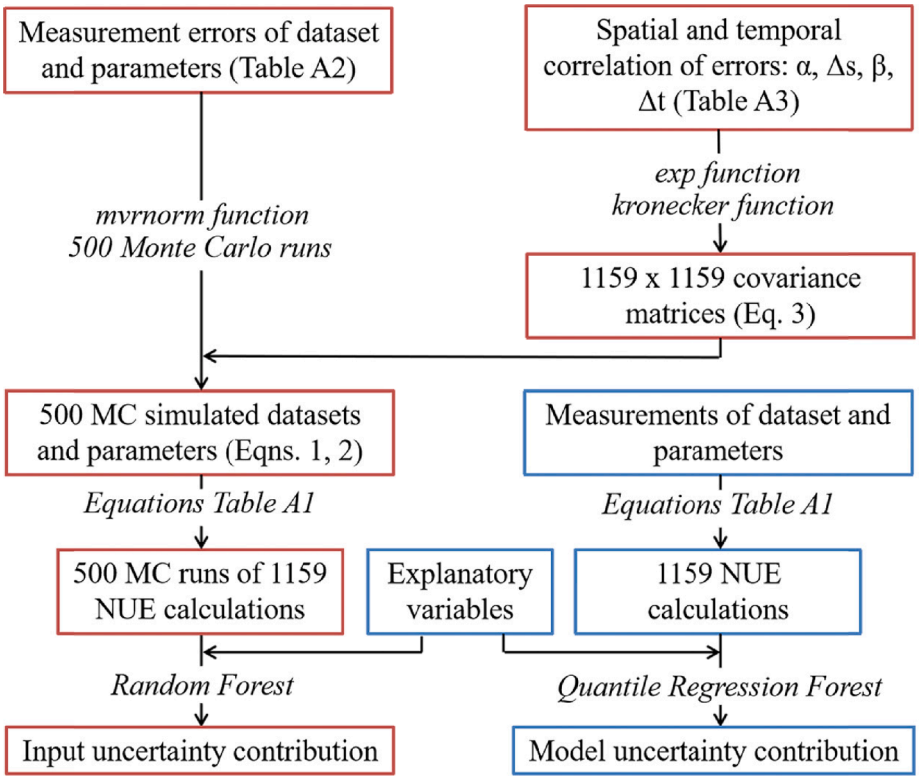

Fig. 1. Flowchart with key steps of the nitrogen use efficiency uncertainty analysis.

defendable because of the central limit theorem (Burt et al., 2009, Section 6.5).

- The means (i.e., expected values) of the error distributions were assumed to be zero in all cases. In other words, it was assumed that there were no systematic measurement errors over the provinces and years.
- With the above two assumptions, the marginal distribution of a measurement error is completely specified once the standard deviation of the distribution is known. In this case, the standard deviations were assumed to be proportional to the measured value.
- Errors between different inputs (such as between yield and N removal) were uncorrelated.
- Measurement errors of the inputs were allowed to be spatially autocorrelated and characterized by a negative exponential function of the geographic distance between the centroids of the provinces.
- Temporal autocorrelation of measurement errors was also incorporated; this was represented by a negative exponential function of the time difference in years.

2.2.2. *Quantifying the standard deviation of input errors*

As mentioned above, the standard deviation of the input errors was assumed to be proportional to the measured value:

$$\sigma_{ijk} = \frac{PE_{ijk}}{100\%} \cdot Y_{ijk} \quad (2)$$

Here, σ_{ijk}, PE_{ijk} and Y_{ijk} are the standard deviation, the proportional error (expressed as a percentage) and the measured value for province i, year j and input k, respectively.

The input errors mainly refer to errors in crop yield, N removal and N input. Specifically, N removal was calculated from yield and N requirement for each crop. However, the N requirement and its uncertainty may be different for different crop varieties. The uncertainty of N requirement in the reference scenario was derived from He et al. (2018), which summarized mean values and standard deviations of N requirement from previous publications. The N input was obtained by aggregating N from chemical fertilizer, manure, cake fertilizer and straw return. Each of these components was calculated by the equations given in Table A1, with corresponding parameters given in Table A2. For example, the chemical fertilizer as one of the N inputs, was composed of single N fertilizer and N from compound fertilizer (Table A1). Due to the N proportion in compound fertilizer being different between diverse fertilizer companies and brands among different years, different parameters were used for different regions and years. The proportional error (PE) of single N fertilizer and compound fertilizer was derived from "N input", while the PE from N ratio in compound fertilizer was derived from the "N input coefficient" (Table A2). Manure, as the second N input, included even more parameters: the number of human and livestock species, the amount of N content in excretion and urine per year (i.e., daily excretion/urine, N content, population structure, and feeding period) and the returning rate to field (Table A1). To simplify the calculations, "manure coefficient" from "N input coefficient" were taken to represent the aggregated parameters of manure (i.e., the amount of N content in excretion and urine and returning rate to field) (Table A2).

Generally, activity data collected from official statistics or from first-hand measurements have a smaller PE (likely between 2.5 and 10 %) (e.g., crop yield, animal numbers, single N fertilizer application amount) (Huang et al., 2012; Gu et al., 2015; Luo et al., 2019; Xu et al., 2019) than activity data and parameters collected or summarized from published studies, which have a larger PE range (0.3 – 80 %) (e.g., N requirement, N input) (He et al., 2018). Note that the PE can be different between crops, years and provinces.

The PE in the optimistic and pessimistic scenarios were chosen as half and double the PE values of the reference scenario, respectively. Due to the large differences among the water content of sugar crops, vegetables, fruits and melons, the uncertainty of these crops was assumed to be larger (i.e., double) than for dry matter crops, such as cereals and oil crops. Cereal yield information was obtained from a complete survey for the period before 1989. Therefore, the PE of cereal yield was assumed to be small (i.e., 5 % for the reference scenario),

while other crops with dry matters had a larger PE (i.e., twice as large as cereal crops: 10 % for the reference scenario). Sugar crops, vegetables, fruits, melons had a twice as large PE than dry matter crops, as mentioned before. From 1989 onward sample survey data were used that obtained from National Bureau of Statistics of China in 2019 (https://data.stats.gov.cn). Therefore, the cereal yield uncertainty was larger than before, which was influenced by sample quality and planting area (because total production is the product of sample yield and planting area). In addition, the improvement of statistical methods and laws decreased the uncertainty of statistical data over the years. The statistics law of the People's Republic of China has been enacted in 1983, and amended in 1996, 2009. Based on this, PEs were decreased for more recent years. For instance, the PE of dry matter crops from 1989 to 1996 (8 % for the reference scenarios) was smaller than in 1978–1988, but note that it was larger than that of cereal crops in the previous period, because the latter was based on a complete survey. The quantification of the PEs relied largely on expert judgement, which is not as reliable as a quantitative assessment of measurement errors. Therefore, three scenarios were used to quantify the uncertainty of measurements of yield, N removal and N input: Optimistic (O), Reference (R) and Pessimistic (P) (see Table A2). Comparison of results between these scenarios provides insight into how sensitive the results of the uncertainty propagation analysis are to the values of the PEs.

2.2.3. Spatial and temporal correlation of the errors

Uncertainty about spatially distributed input data tends to be positively spatially correlated, and this influences the degree to which uncertainties cancel out by spatial aggregation (Kros et al., 2012). The uncertainty about input data might also be positively correlated over time, since in adjacent years the same errors can be repeated by using the same tools, methods or operators to measure or collect data. Spatial and temporal autocorrelation of the measurement errors was represented by a negative exponential function:

$$\rho(\Delta s, \Delta t) = e^{-\alpha \cdot \Delta s - \beta \cdot \Delta t} \quad (3)$$

where Δs and Δt refer to distance in space in kilometers and distance in time in years, respectively. The centroids of provinces were used to determine the distances between provinces. Three scenarios were used, because the parameters α and β could only be derived by expert judgement (Table A3). For each scenario α and β were assumed to be the same for all uncertain inputs.

With defining the PEs and spatial and temporal autocorrelation functions, the joint distributions of all uncertain inputs were fully characterized. The vector of all input errors had a multivariate normal distribution, whose mean vector was zero and whose variance–covariance matrix could be derived from the autocorrelation functions, the PE values given in Table A2, and the measured inputs. Since no cross-correlation was assumed between uncertain inputs, the joint normal distributions for each input could be managed separately. Note that the joint distribution was still complex, because the vector of normal variates for each input consisted of 1159 elements. The 1159 × 1159 covariance matrices were derived for all inputs as described above and it was verified that all were positive-definite.

2.3. Uncertainty propagation

2.3.1. Propagation of input uncertainty

Monte Carlo method

The Monte Carlo method is by far the most often used tool for uncertainty propagation analysis since it is transparent, easily implemented and generally applicable (Heuvelink, 1998a; Sonnemann et al., 2003; Liu et al., 2017; Jiao et al., 2019). It can approximate the probability distribution of the uncertain output at an arbitrary accuracy level as long as the number of Monte Carlo simulations is large enough (Heuvelink, 1998b). The Monte Carlo approach starts by sampling a large number of 'possible realities' from the probability distributions of the uncertain inputs, using a pseudo-random number generator. In this study, 500 Monte Carlo runs were used, which is considered sufficient to reach stable results (Heuvelink, 1998a, Section 4.2; Nol et al., 2010). As the joint distribution of the uncertain inputs was multivariate normal, the *mvrnorm* function of the *MASS* package (version 7.3–54) in R could be used (Venables and Ripley, 2002). Note that negative simulations were set to zero.

2.4. Propagation of input uncertainty to NUE calculations

The yields of all crops were summed for each Monte Carlo run to get the total yield of each province and year for that run. The same was done for N removal. N input was already recorded for total crops, hence summation for all crops was not needed.

The PFP_N and PNB_N values for each Monte Carlo run were next computed from the yield, N removal and N input simulations for each province and year. The frequency distributions of the 500 values of PFP_N and PNB_N represent the propagation of input uncertainty to uncertainty in NUE calculations. In particular, the width of these distributions (in this study characterized by the difference between the 0.95 and 0.05 quantiles) signifies the uncertainty of the calculated NUE indicator.

2.5. Random forest model

The RF model, developed by Breiman (2001), tends to have higher accuracy compared with other machine learning approaches (Hengl et al., 2015). It belongs to the family of ensemble machine learning algorithms that predicts a dependent variable (i.e., a NUE indicator) from a set of explanatory variables selected randomly using a bootstrapping technique (sampling with replacement). Once a model is calibrated using paired observations of the dependent and explanatory variables (the training data), it is used to predict the dependent variable from only the explanatory variables. The explanatory variables used to build the RF model included crop type, topography, soil, climate, economy and agricultural management practice (AMP). These were obtained from the Climatic Research Unit (1978–2015, https://www.cru.uea.ac.uk/data), Harris et al. (2014), National Bureau of Statistics of China during 1978–2015 (https://data.stats.gov.cn) and published articles (Shangguan et al., 2014; Hengl et al., 2017; Poggio et al., 2020). More details about the explanatory variables are provided in Liu et al. (2020b). All explanatory variables available as raster maps were aggregated to provincial scale by taking the spatial average over all raster cells within a province. Crop and soil types were transformed to continuous-numerical variables by computing area proportions. Annual temperatures at night and daytime were also included. In summary, there were 1159 NUE observations (30 provinces from 1978 to 2015; Chongqing province was established in 1997) and 108 explanatory variables.

2.6. Propagation of input uncertainty through the NUE random forest model

After obtaining the 500 PFP_N and PNB_N Monte Carlo simulations for each province and year, the RF model was fitted for each case, i.e., 500 different RF models were obtained because each model was calibrated with a different PFP_N and PNB_N dataset. The differences between the models and their predictions showed how measurement uncertainty in inputs propagated to the model output. The uncertainty in RF predictions was characterized by the 90 % prediction interval width (PIW_{90}) and the ratio of the inter-quantile range over the median (prediction interval ratio, PIR_{90}). Note that these uncertainty metrics were computed for every province and year. Their equations are as follows (Poggio et al., 2020):

$$PIW_{90} = q_{0.95} - q_{0.05} \quad (4)$$

$$PIR_{90} = \frac{q_{0.95} - q_{0.05}}{q_{0.50}} \quad (5)$$

Here, $q_{0.05}$, $q_{0.50}$ and $q_{0.95}$ are the 0.05 quantile, median and the 0.95 quantile of the 500 NUE predictions, respectively.

2.6.1. Model uncertainty

The RF model also causes uncertainty, because the explanatory variables cannot explain all of the variation of the NUE indicators. For instance, the RF model could explain only 84 and 89 % of the variation of PFP_N and PNB_N, respectively in the study of Liu et al. (2022).

The QRF in this study was used to quantify the model uncertainty (Meinshausen, 2006). QRF is similar as RF, but it gives a non-parametric estimation of the quantiles of the conditional distribution of the dependent variables (i.e., NUE indicators). It keeps the value of all observations in each node of each tree of the random forest, not just their mean, and assesses the conditional distribution based on this information. It is invoked in the *ranger* function of the *ranger* package (version 0.13.1) in R, with *quantreg* option set to TRUE. In this case, the prediction is not a single value, i.e., the average of the predictions from the group of decision trees in the random forest, but a cumulative probability distribution of the PFP_N and PNB_N for each province and year. The 0.05, 0.50 and 0.95 quantiles from this distribution were obtained to compute the PIW_{90} and PIR_{90} associated with model uncertainty.

2.7. Uncertainty sources contributions

Both input uncertainty and model uncertainty lead to uncertainty in RF predictions of NUE indicators. Previous sections explained how these uncertainties can be derived by using Monte Carlo simulation for input uncertainty and QRF for model uncertainty. The magnitude of the uncertainties was quantified with PIW_{90} and PIR_{90}. Once these are obtained it is an easy step to compare them. The uncertainty contributions of each source were computed by dividing each by the sum. Such analysis can provide highly relevant information. For instance, if input uncertainty is the principal uncertainty source (with larger PIW_{90} or PIR_{90}), then it is important to improve the accuracy of the yield data, human and livestock numbers, chemical fertilizer data and corresponding coefficients. If model uncertainty is the main uncertainty source, then there is little gain in putting a large effort in collecting more accurate data and coefficients. Instead, improvements can best be achieved by obtaining more and better explanatory variables and models. Note that the uncertainty contributions were computed for all provinces and years and can be different between provinces and years.

3. Results

This section only presents results of the uncertainty analysis. Spatial patterns and time series of PFP_N and PNB_N calculations and RF model predictions are given in Liu et al. (2020b) and Liu et al. (2022). Due to space limitations, results are only presented for three provinces (Heilongjiang, Henan and Sichuan) and the year 2015. Results for other provinces and the entire period are presented in the Appendix. The three provinces were selected due to fact that they are main food productive provinces in China and their different environmental conditions and geographical locations are fairly representative for the whole of China.

3.1. Uncertainty of NUE calculations for different scenarios

The probability distribution width (i.e., difference between the 0.95 and 0.05 quantiles) was used to describe the uncertainty of PFP_N and PNB_N calculations for each province and year. Results showed as expected that the uncertainty of PFP_N and PNB_N calculations in the reference scenario was larger than that in the optimistic and smaller than that in the pessimistic scenario (Figs. A1 and A2). For PFP_N, Guangxi and Shanghai had the largest distribution width (19 and 14 kg kg^{-1} in reference scenario, respectively), while Jilin and Inner Mongolia had the smallest distribution width (both were 4 kg kg^{-1} in the reference scenario, see Fig. A1). For PNB_N, Heilongjiang and Jilin had the largest distribution width (0.3 and 0.2 kg kg^{-1} in the reference scenario, respectively), while Beijing and Hainan had the smallest distribution width (both were 0.06 kg kg^{-1} in reference scenario, see Fig. A2). All distributions had small skewness and did not deviate much from normal distributions.

3.2. Propagation of input calculations uncertainty to RF model output

As explained in Section 2.3, the 500 PFP_N and PNB_N calculations obtained with the Monte Carlo method and presented in Section 3.1 were used to calibrate 500 RF models to assess the propagation of input errors through the RF model. This was again done for the three scenarios and for all provinces and years. In this section time series and spatial maps of the uncertainties of these RF model outputs are presented and interpreted.

3.2.1. PFP_N uncertainty

The magnitude and temporal variations of PFP_N prediction uncertainty in Heilongjiang, Henan and Sichuan provinces are shown in Fig. 2 (PIR_{90}) and A5 (PIW_{90}). Overall, the PIW_{90} in the three provinces decreased with time until 2000, after which it was stable in Heilongjiang and increased in Henan and Sichuan (Fig. A5). The PIW_{90} was higher in Heilongjiang than in the other two provinces before 2005. The PIR_{90} in Heilongjiang and Henan had a decreasing trend while it decreased before and increased after 2000 in Sichuan (Fig. 2). The PIR_{90} was largest in Heilongjiang and smallest in Sichuan in 1978, while it was the converse in 2015. The temporal variation of PFP_N prediction uncertainty in 31 provinces in China is shown in Figs. A5 (PIW_{90}) and A6 (PIR_{90}). The temporal variation of PIW_{90} was different in different provinces and most provinces had a decreasing trend before 2000, after which it increased or stayed stable, except for Tianjin, which had a decreasing trend (Fig. A5). The PIR_{90} in most provinces had a declining trend over time (Fig. A6).

The spatial variation of PFP_N prediction uncertainty in Heilongjiang, Henan and Sichuan is shown in Fig. 3 (PIR_{90}) and A7 (PIW_{90}). PIR_{90} was higher in south and west China than in other regions in 2015 (Fig. 3). In 2015, PIR_{90} was lower than 0.10 in the optimistic scenario (Fig. 3a); between 0.10 and 0.20 in the reference scenario for most provinces, except for Heilongjiang, where it was 0.09 (Fig. 3b); and between 0.20 and 0.40 in the pessimistic scenario (Fig. 3c). For PIW_{90}, south and east-coastal China had higher values than in other regions in 2015 (Fig. A7). In 2015, the PIW_{90} of most provinces in the optimistic scenario were smaller than 5 kg kg^{-1} yr^{-1}, except for Guangxi. In addition, it was lower than 10 kg kg^{-1} yr^{-1} in the reference scenario, except for Guangxi and Shanghai (Fig. A7b). As expected, the largest uncertainty of PIW_{90} occurred in the pessimistic scenario (7 – 28 kg kg^{-1} yr^{-1}) (Fig. A7c).

3.2.2. PNB_N uncertainty

The magnitude and temporal variation of PNB_N prediction uncertainty for the three input uncertainty scenarios in Heilongjiang, Henan and Sichuan is shown in Fig. 4 (PIR_{90}) and A8 (PIW_{90}). The PIW_{90} in Heilongjiang, Henan and Sichuan generally decreased over time. After 2000 it increased dramatically in Heilongjiang and increased slightly in Henan and Sichuan. Overall, the PIW_{90} was higher in Heilongjiang and smaller in Sichuan than in Henan (Fig. A8). The PIR_{90} showed a downward trend in Henan and Sichuan and fluctuations in Heilongjiang, but it went up after 2000. The PIR_{90} in Heilongjiang was smaller than in the other two provinces before 2000, and higher after 2000. It should be noted that Sichuan had a higher PIR_{90} than Henan all the time (Fig. 4). The temporal variation of PIW_{90} and PIR_{90} in 31 provinces for PNB_N was similar to that for PFP_N (Figs. A8 and A9).

For PNB_N, the PIR_{90} in 2015 was higher in northeast China than in other regions (Fig. 5). The PIR_{90} of most provinces in the reference

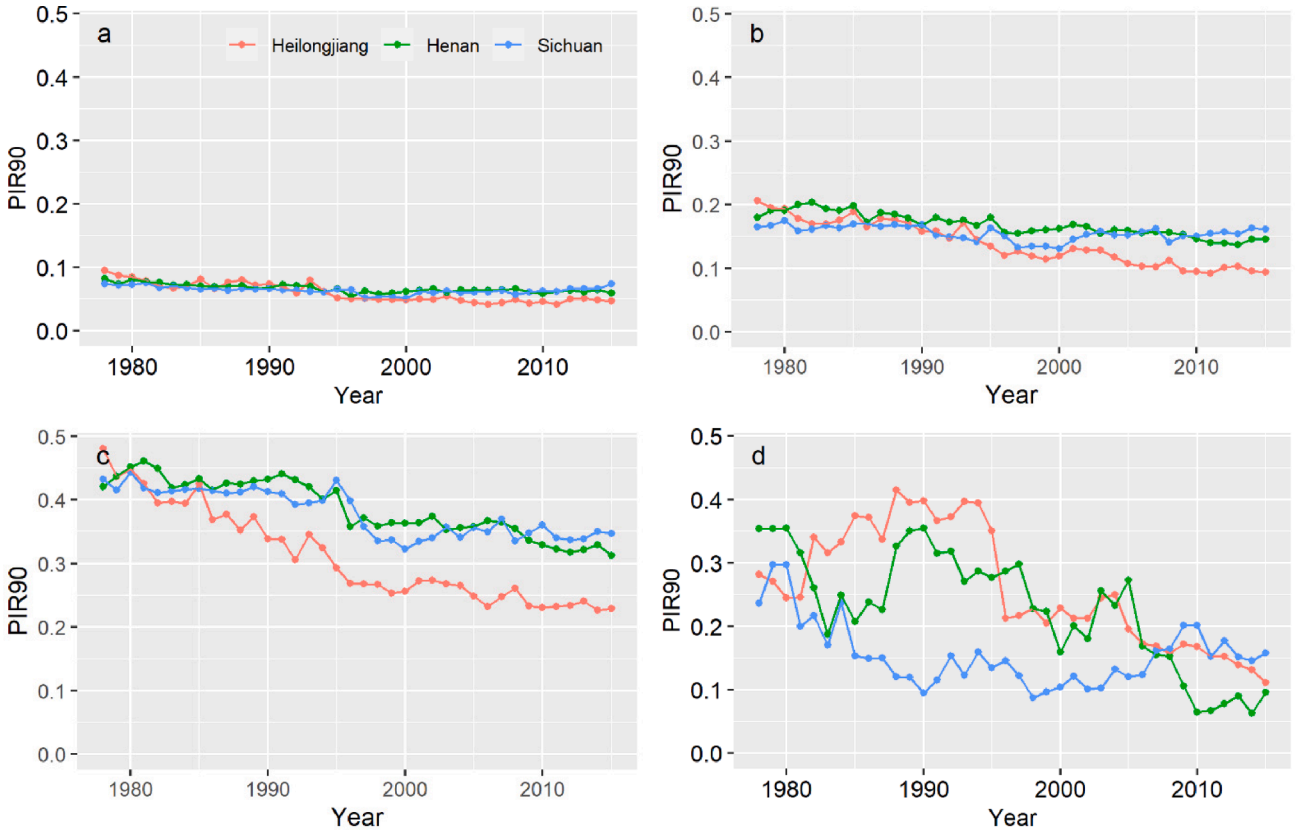

Fig. 2. Time series from 1978 to 2015 of the partial factor productivity (PFP_N) 90% prediction interval ratio (PIR_{90}) of the random forest model outputs in Heilongjiang, Henan and Sichuan, as resulting from measurement uncertainty in input data for the optimistic (a), reference (b), and pessimistic scenarios (c), and as resulting from model uncertainty (d).

scenario was between 0.1 and 0.2. In the pessimistic scenario, most provinces had a PIR_{90} within 0.2 and 0.5, apart from Jilin, Inner Mongolia, Liaoning and Heilongjiang. The PIW_{90} of different scenarios had similar spatial distribution patterns as PIW_{90} in 2015 (Fig. A10). In 2015, the PIW_{90} of most provinces in the optimistic scenario were smaller than 0.1 kg kg^{-1}. It was also lower than 0.1 kg kg^{-1} in the reference scenario, except for Heilongjiang, Jilin and Inner Mongolia. It was between 0.1 and 0.3 kg kg^{-1} in the pessimistic scenario, except for Hainan, Heilongjiang and Jilin.

3.3. Model uncertainty

3.3.1. PFP_N model uncertainty

The PIW_{90} of the QRF model in Heilongjiang was higher than that in the other two provinces (Fig. A5d). It was higher in Henan than in Sichuan from 1978 to 2008, but reversed from 2008 to 2015. For PIR_{90}, Heilongjiang had considerably higher values than Henan and Sichuan during 1982–1995 (Fig. 2d). Henan had a lower model uncertainty PIR_{90} than Sichuan from 2007 onwards. The temporal variation of model uncertainty (PIW_{90} and PIR_{90}) had more fluctuations than that of input uncertainty (Figs. A5 and A6). Note that the uncertainty resulting from model uncertainty was higher than that obtained in the optimistic and reference input error scenarios, but smaller than that of the pessimistic input error scenario (see also Section 3.4). The PIR_{90} for the QRF model in northwest and east China was higher than in other regions in 2015 (Fig. 3d). The PIW_{90} was higher in northwest and southeast China in 2015 (Fig. A7d).

3.3.2. PNB_N model uncertainty

The PIW_{90} for the QRF model in Heilongjiang was higher than in other provinces (Fig. A8d). It was higher in Henan than in Sichuan from 1978 to 2008, but reversed from 2008 to 2015. Heilongjiang and Henan had higher PIR_{90} than Sichuan before 1995, and thereafter Heilongjiang had similar PIR_{90} as Sichuan, while Henan had the lowest PIR_{90} (Fig. 4d). The model uncertainty (PIW_{90} and PIR_{90}) had a decreasing trend over time and showed more fluctuations than uncertainty caused by input measurements (Figs. A8 and A9). The PIR_{90} in 2015 was higher in north China than in south China in 2015 (Fig. 5d). For PNB_N, the PIW_{90} of the QRF model was highest in north and west China in 2015 (Fig. A10d).

3.4. Uncertainty source contributions

The NUE uncertainty was caused by input measurement uncertainty and model uncertainty. This section compares the contributions of these two uncertainty sources for the reference scenario case, and using PIR_{90} as uncertainty metric. Figs. 6, 7 and A11 show the input uncertainty contributions, presented as a percentage of the total uncertainty (i.e., the sum of the PIR_{90} of both sources). Input uncertainty is the dominant source of uncertainty if it is above the horizontal dashed lines in Figs. 6 and A11, otherwise model uncertainty has a bigger contribution.

3.4.1. Uncertainty sources contribution for PFP_N

The input uncertainty contribution in Heilongjiang was higher than in Henan and Sichuan until 1981, after which it was lower than in the other provinces (Fig. 6a). The input uncertainty contribution in Sichuan was higher than in Henan at first but after 2008 it was lower than that in Henan. The input uncertainty contribution in Heilongjiang was smaller than the model uncertainty contribution during the entire period from 1980 to 2015, while Sichuan and Henan had an input uncertainty contribution higher than 50 % in the 1985–2006 and 2008–2015 periods, respectively. The contributions of input uncertainty were within

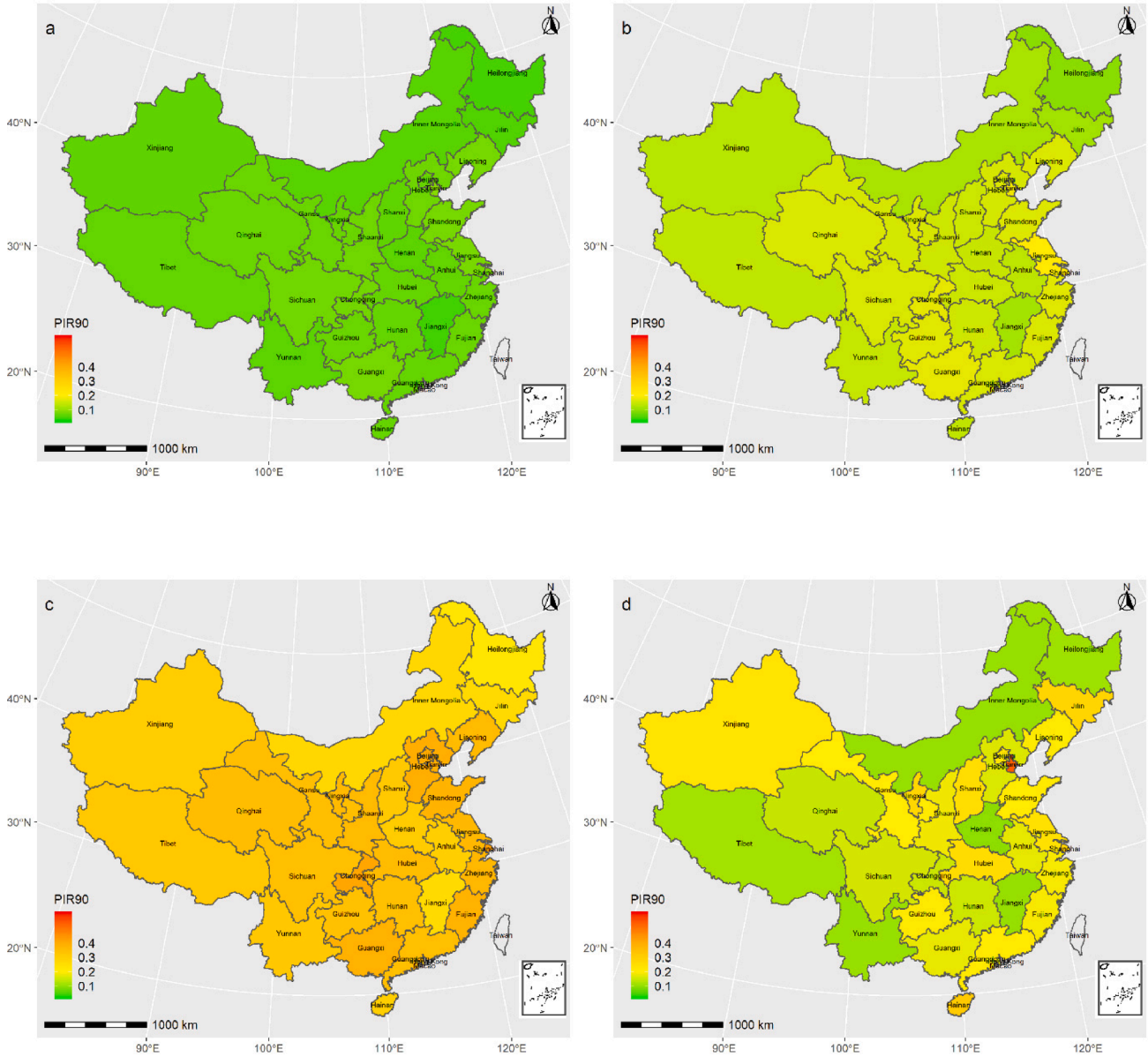

Fig. 3. Spatial distribution of the 90% prediction interval ratio (PIR_{90}) of PFP_N in 31 provinces of China in 2015, in the optimistic (a), reference (b) and pessimistic scenarios (c), obtained by propagating measurement uncertainty in crop yield, N removal and N input measurements through the RF model. Map of PIR_{90} caused by model uncertainty as quantified by quantile regression forests (d).

25 and 60 % from 1978 to 2015 for most provinces; most provinces had an input uncertainty contribution smaller than 50 % (Fig. A11a). There was also a large variation in spatial patterns of input uncertainty contribution. In 2015, the input uncertainty contribution in Henan, Yunnan and Tibet was higher than 55 %, while Tianjin and Jilin had the smallest values (<30 %) (Fig. 7a).

3.4.2. *Uncertainty sources contribution for PNB_N*

The input uncertainty contribution in Sichuan was higher than in other provinces before 1995, and lower than in other provinces after 2009 (Fig. 6b). The temporal variation trend of input uncertainty contribution in Henan and Heilongjiang was very similar: fluctuating and on average upward. The input uncertainty contribution in Sichuan was close to or higher than 50 % over time, while Henan and Heilongjiang mostly had input uncertainty contributions higher than 50 % after 1995. The contributions of input uncertainty were within 30 and 60 % in 1978 for most provinces and increased to the range of 40 – 75 % in 2015; most provinces had input uncertainty contributions lower than 50 % before 2010 (Fig. A11b). Large variation existed in the spatial distribution of input uncertainty contribution (Fig. 7b). In 2015, the input uncertainty contribution in Jiangxi, Henan, Guangxi and Heilongjiang was higher than 66 %, while it was lower than 40 % in Tianjin, Beijing and Qinghai (Fig. 7b).

4. Discussion

4.1. *Uncertainty of NUE predictions*

Most of the uncertainty assessment of input data was based on expert knowledge and unreliable. This problem was addressed quantitatively by using three scenarios. The results indicated that the uncertainties are different in different scenarios, which meant that the results of the uncertainty analysis are sensitive to the quantification of input uncertainty. Therefore, it is important that the government pays more attention to accurate assessment of input uncertainty. Moreover, yield aggregation at spatial and crop scale leads to additional input uncertainty. Porwollik

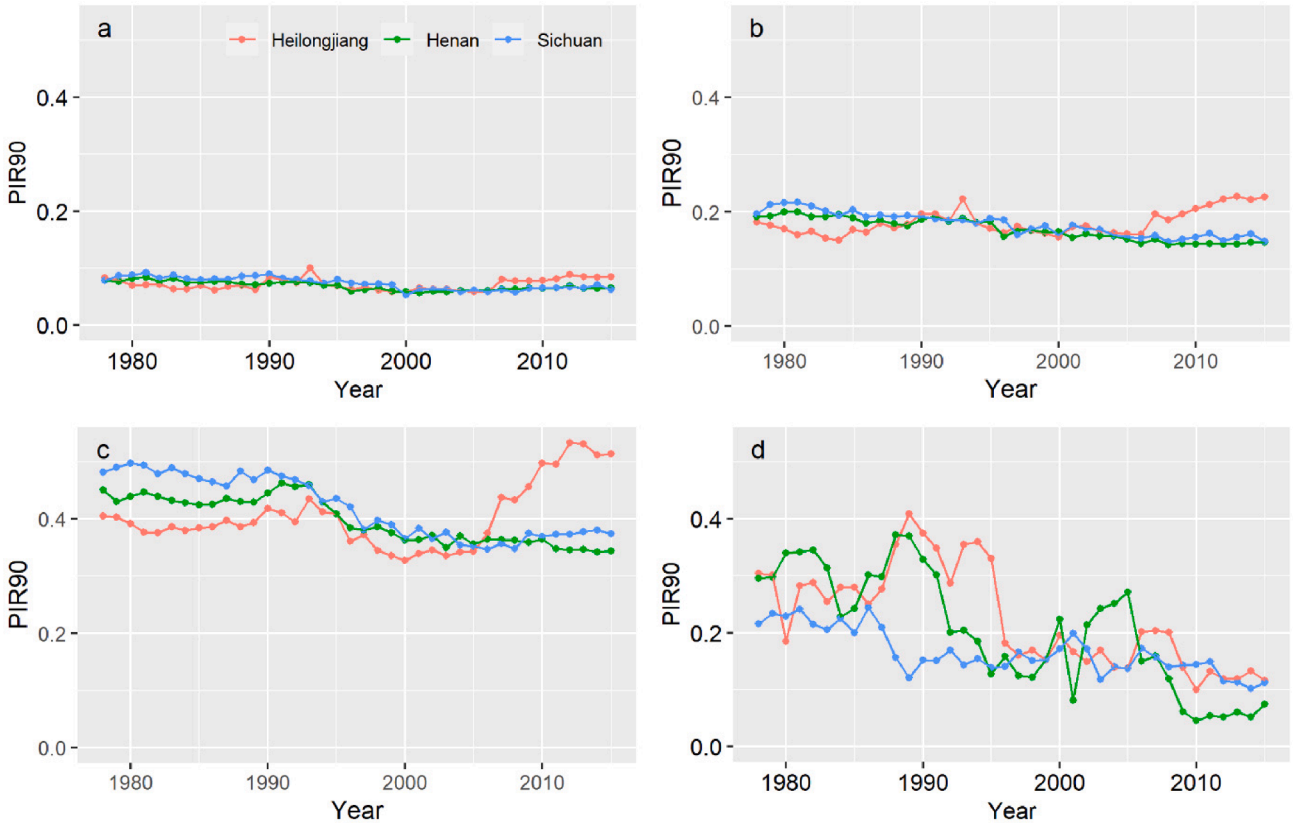

Fig. 4. Time series from 1978 to 2015 of the 90 % prediction interval ratio (PIR_{90}) of PNB_N for Heilongjiang, Henan and Sichuan in the optimistic (a), reference (b), and pessimistic scenario (c), obtained by propagating measurement uncertainty in crop yield, N removal and N input measurements through the RF model. Times series of PIR_{90} as caused by model uncertainty and quantified by quantile regression forests (d).

et al. (2017) demonstrated that aggregation uncertainty of gridded yields at national scale can be up to 37 % (maize, in South Africa), 43 % (wheat, in Pakistan), 51 % (rice, in Japan), and 427 % (Soybean, in Bolivia). On the other hand, crop aggregation leads to uncertainty of provincial yield, since there are large differences between dry matter crop yield and fresh weight crop yield. Zhang et al. (2021a) reported that uncertainties of N inputs and outputs were 8 % and 12 %, respectively. Chemical fertilizer, as the most important N input, is uncertain because of uncertainty in fertilizer rate collected and N ratio in compound fertilizer. For manure, process wastewater was the dominant source of uncertainty in manure application N, contributing 64 – 94 % to the overall uncertainty (Miller et al., 2020). Other uncertainty might arise from N content in manure and livestock numbers. These parameters used in the calculations lack validation and may have large uncertainty.

Interestingly, model uncertainty had similar spatial and temporal trends as input uncertainty. A possible explanation is that the development of science and technology improve the accuracy of input data and model simultaneously. Temporal variation of model uncertainty had more fluctuations than input uncertainty during the study period. This might be because the annual discrepancies in some explanatory variables were neglected due to lack of information. This leads to a weaker relation between the target variable (i.e., NUE) and explanatory variables, which means a higher model uncertainty in time. But it is difficult to determine which explanatory variables cause this effect since the QRF model is a highly complex model in which it is difficult to see the effect of each variable on the predictions. Wang et al. (2017) and Lobell and Field (2007) indicated that the uncertainty of temperature measurement or prediction will influence the accuracy of crop yield prediction. Additionally, the explanatory variables could not explain all variation in NUE indicators because crucial explanatory variables were lacking, such as fertilizer management information. Model uncertainty also increased because no information about water supply was available, which is known to have a significant influence on NUE indicators (Lemaire and Ciampitti, 2020). Helfenstein et al. (2022) and Hounkpatin et al. (2022) indicated that the QRF model may slightly overestimate the prediction uncertainty. Therefore, other advanced models might be applied in order to find a more suitable model for NUE uncertainty. Nigon et al. (2020) showed that the performance among *Lasso, SVR, and PLSR* was comparable when predicting N requirement in maize, while the performance of random forest was substantially inferior with higher error values.

The temporal and spatial variation of NUE uncertainty (PIW_{90}) (Figs. A5, A7, A8 and A10) from uncertainty in input data was related to the variation of PFP_N values as shown in Fig. 2a in Liu et al. (2020b). This phenomenon was most obvious in the pessimistic scenario. A possible reason for this is that the assumption for parameters/statistical data for computing input data (crop yield, N removal and N input) was based on proportional errors. This effect shows up in the PIW_{90} but not in the PIR_{90}, because PIR_{90} is a relative error metric (with the median in the denominator).

Overall, PIR_{90} decreased over time. This may be explained from the improvement of technology and statistical policy over the years. A very interesting result was that northeast China had a lower PIR_{90} for PFP_N, but a higher PIR_{90} for PNB_N in 2015. Since these were calculated by the same N input, the difference can only be explained from differences in crop yield and N removal uncertainties. An explanation is that the uncertainty of crop yield was lower in northeast China, while N removal uncertainty was higher in northeast China (Fig. A12). That might be caused by the crop types that are different between these regions. Northeast China has much less fruits, vegetables and melons, which were high yield uncertainty crops.

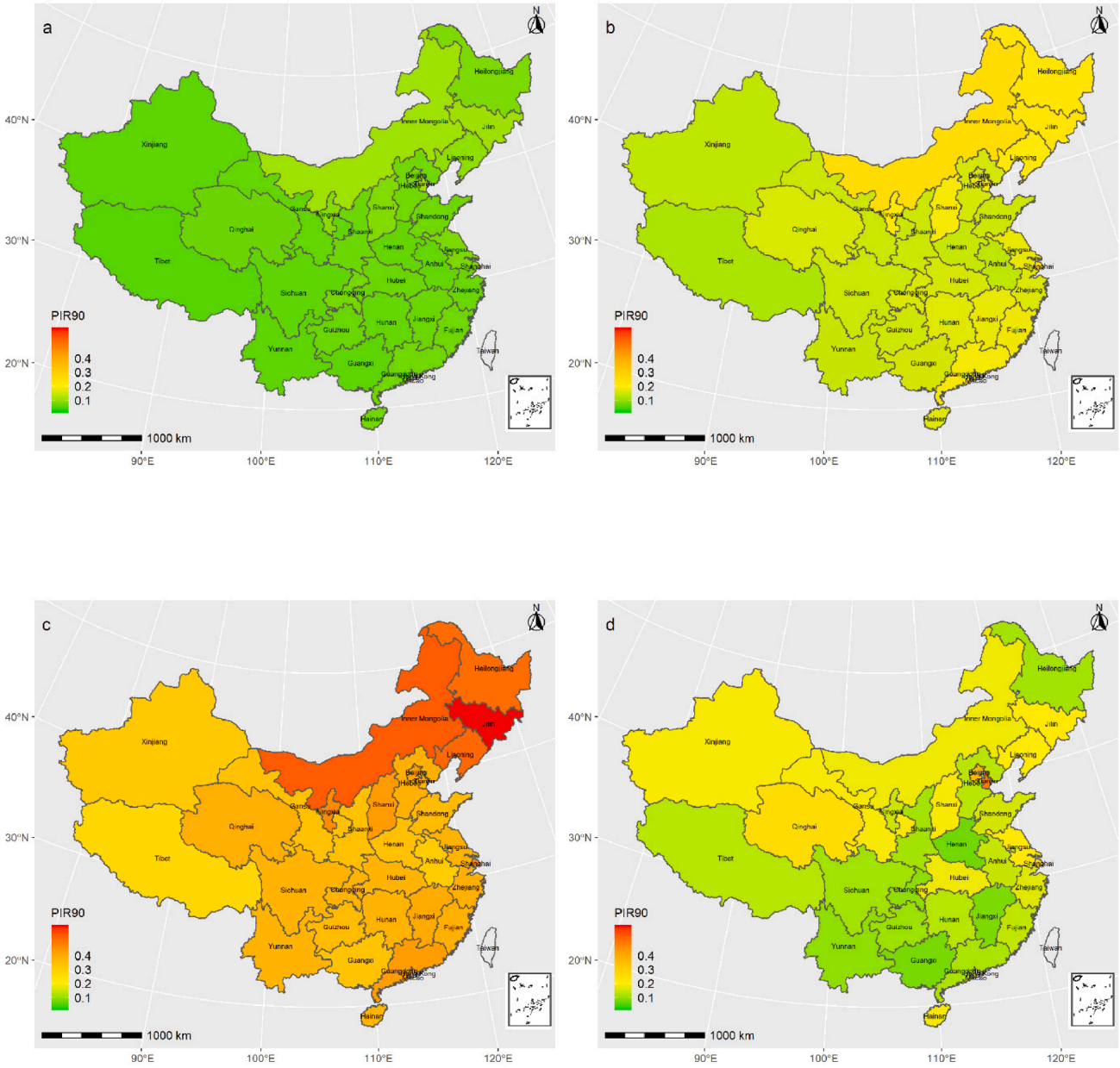

Fig. 5. Spatial distribution of the 90 % prediction interval ratio (PIR_{90}) of PNB_N in 31 provinces of China in 2015, in the optimistic (a), reference (b) and pessimistic scenarios (c), obtained by propagating measurement uncertainty in crop yield, N removal and N input measurements through the RF model. Map of PIR_{90} caused by model uncertainty as quantified by quantile regression forests (d).

4.2. Contribution of uncertainty sources to NUE prediction uncertainty

In this study, the input uncertainty contribution in the reference scenario had a similar distribution range for PFP_N and PNB_N. Overall, input uncertainty had lesser contribution than model uncertainty in most of the provinces, except for PNB_N after 2010 (Fig. A11) and the contribution of input uncertainty increased over time, possibly because the QRF model improved over time. This also meant that the QRF model was more competitive for PNB_N in the 2010s. More attention should be paid to improving the accuracy of explanatory variables or the advancement of models to decrease the model uncertainty propagation to PFP_N, while simultaneously improving the input data accuracy when computing PNB_N. Both investments pay off because both sources of uncertainty have a substantial and comparable contribution.

It is worth noting that Tianjin and Jilin had smaller input uncertainty for PFP_N. In other words, in these cases the model uncertainty was most limiting. More suitable models need to be applied in these provinces if more explanatory variables cannot be collected to improve model performance. For PNB_N, provinces in south and northeast China had higher input uncertainty than model uncertainty. This might be because N removal had larger uncertainty in northeast China with higher uncertainty crops (e.g., rice, maize). Moreover, there are more crop types and planting seasons in south China, which leads to high uncertainty in N removal and N input. Del Grosso et al. (2010) showed that model uncertainty and input data accounted for 83 % and 17 % of the total uncertainty of N_2O emission, respectively. In such case, it is best to put more effort in model improvement. In this study, both uncertainty sources had large contributions in the recent past. Therefore, it is advised to put more effort into obtaining reliable information about statistical data and crop parameters as well as improving the model performance.

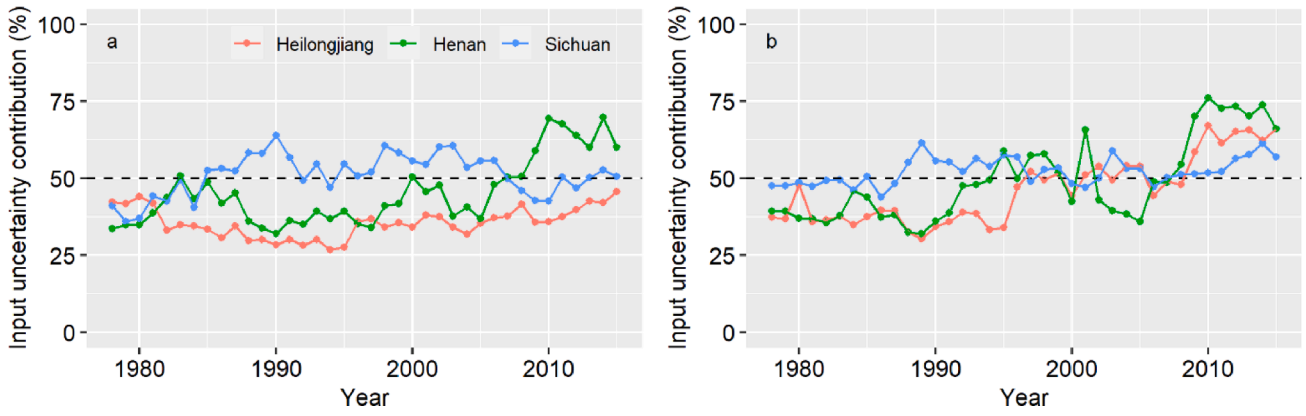

Fig. 6. Time series from 1978 to 2015 of input uncertainty contributions (90 % prediction interval ratio in reference scenario) of PFP_N (a) and PNB_N (b) in Heilongjiang, Henan and Sichuan. Dashed line represents a case in which input uncertainty and model uncertainty have equal contribution.

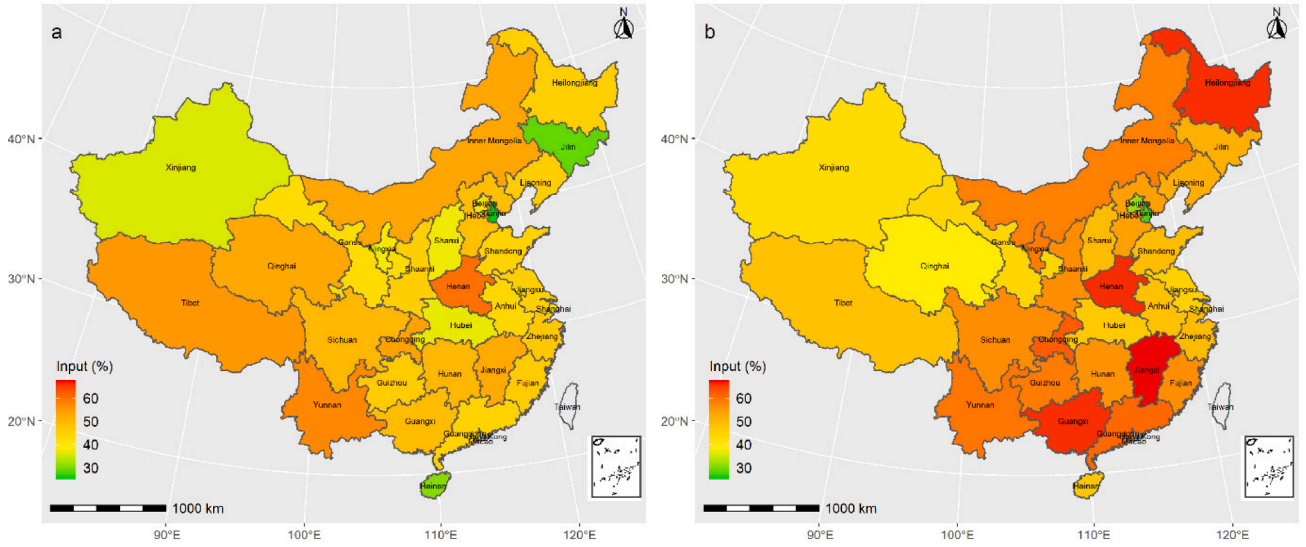

Fig. 7. Spatial distribution of input uncertainty contributions (90 % prediction interval ratio in reference scenario) for PFP_N (a) and PNB_N (b) in 31 provinces in 2015.

4.3. Recommendations for reducing NUE prediction uncertainty

4.3.1. Importance of reducing NUE uncertainty

NUE is an important indicator of scientific and efficient fertilization. Quantifying NUE prediction accurately is beneficial for improved fertilization and mitigating environmental pollution. If NUE indicators can be accurately calculated and predicted, then the optimal N fertilizer rate and fertilization tactics can be better determined. Thus, accurate information about NUE can enhance productivity of crops and decrease fertilization costs of farmers (Lobell, 2007). Meanwhile, the fertilization model can be developed and optimized. Wang and Zhou (2014) indicated that suitable NUE calculation methods could decrease NUE uncertainty and were favorable to guiding fertilization and management. Such analyses could prevent excessive N application and waste of N resources in China. Reducing NUE uncertainty is also helpful to preventing environmental pollution and taking alleviation measures. For example, even though the PNB_N is higher in northeast China than in other parts of the country (Liu et al., 2020b), its uncertainty is also higher in this area. Therefore, it is not certain that northeast China has less environmental pollution. The NUE prediction uncertainty in northeast China should be reduced, using strategies outlined before and in Section 4.3.2 below.

4.3.2. Recommendations for decreasing NUE uncertainty

Most studies on uncertainty related to crop research assess uncertainty through treatment replications (e.g., coefficient of variation, standard deviation). This assesses the uncertainty about the response of crops to fertilizers, but does not represent uncertainty in measurements (Yang et al., 2017). As far as we know, this study is the first attempt to quantify NUE uncertainty at provincial scale, while including spatial and temporal correlation between measurement errors, which is crucial in regional scale assessments and when aggregating results to national level. But more efforts are still needed to improve the NUE uncertainty sources, both from input data and model. Firstly, it is essential to formulate standard procedures and guidelines for data collection and defining their associated uncertainties, especially for key parameters (e.g., crop N requirement, livestock excretion, crop-specific fertilizer application, N ratio in compound fertilizer). The decreasing uncertainty over time shows the benefit of increasingly mature and rigorous statistical surveys. For provinces with higher input uncertainty, such as Henan, Heilongjiang, Guangxi and Jiangxi, it is suggested to improve the accuracy of N requirement parameters (e.g., rice, maize, vegetables and fruits). Secondly, important management practices need to be recorded, such as irrigation water volume (only including irrigation area so far), manure nutrient content for agriculture, fertilization times, and fertilization date. For example, Jilin, Beijing, Tianjin and Hainan provinces

with higher model uncertainty should record more mechanization and economy covariates (e.g., irrigation water volume, crops price) since these may serve as important covariates in an improved machine learning model. Thirdly, the technological advancement of experimental observations and improved bookkeeping of human activity data must be achieved by the statistical bureau, and be shared publicly in a clear and accessible format, to reduce errors in secondary inputs. Finally, a scientists-farmers network should be built. Scientists should cooperate with farmers and train them to finish the survey accurately and online. They can also provide better management practices for farmers in order to increase NUE. In this case, more accurate field parameters can be obtained, thus enhancing NUE accuracy. Although these recommendations cannot be completely achieved within a short term, these should be put on the agenda to realize them in the long run.

5. Conclusion

This study conducted a comprehensive uncertainty analysis for NUE prediction with consideration of the spatial and temporal correlation of measurement errors in inputs. The differences of NUE uncertainty calculations between scenarios were large, which indicates that accurate quantification of the inputs is important. Results also revealed that the random forest model prediction uncertainty (PIW_{90} and PIR_{90}) had a downward trend over time due to the improvement of technology and policy. In 2015, PFP_N had lower uncertainty and PNB_N had higher uncertainty in northeast China. This was likely caused by the difference in major crop types between these regions. NUE had smaller input uncertainty than model uncertainty in most provinces, except for PNB_N, which showed converse results after 2010. This means that the QRF model had a better performance for PNB_N in the 2010s. Overall, both input and model uncertainties contributed more or less equally to uncertainty in predicted NUE indicators. This indicates that it pays off to invest both in improved input data collection and covariates preparation. Future work should therefore focus on improved bookkeeping of detailed field and survey data and accurate collection of crop parameters and explanatory variables.

CRediT authorship contribution statement

Yingxia Liu: Conceptualization, Data curation, Formal analysis, Investigation, Methodology, Software, Validation, Visualization, Writing – original draft, Writing – review & editing. **Gerard B.M. Heuvelink:** Data curation, Funding acquisition, Methodology, Project administration, Resources, Software, Supervision, Visualization, Writing – review & editing. **Zhanguo Bai:** Conceptualization, Data curation, Investigation, Project administration, Resources, Software, Supervision, Writing – review & editing, Visualization. **Ping He:** Conceptualization, Funding acquisition, Project administration, Resources, Supervision, Writing – review & editing.

Declaration of Competing Interest

The authors declare that they have no known competing financial interests or personal relationships that could have appeared to influence the work reported in this paper.

Data availability

Data will be made available on request.

Acknowledgements

We thank Rong Jiang and Dainius Masiliūnas for their contributions to data collection and code programming. This work was supported by the National Natural Science Foundation of China (No. 31972515) and the Earmarked fund for the China Agriculture Research System (No. CARS-09-P31). We are especially acknowledgeable to financial support from the China Scholarship Council (CSC) [201903250115].

Appendix A. Supplementary data

Supplementary data to this article can be found online at https://doi.org/10.1016/j.compag.2022.107533.

References

Breiman, L., 2001. Random forests. Mach. Learn. 45, 5–32. https://doi.org/10.1023/A:1010933404324.

Burt, J.E., Barber, G.M., Rigby, D.L., 2009. Elementary Statistics for Geographers. Guilford Press.

Córdoba, M., Carranza, J.P., Piumetto, M., Monzani, F., Balzarini, M., 2021. A spatially based quantile regression forest model for mapping rural land values. J. Environ. Manage. 289, 112509 https://doi.org/10.1016/j.jenvman.2021.112509.

Correndo, A.A., Rotundo, J.L., Tremblay, N., Archontoulis, S., Ciampitti, I.A., 2021. Assessing the uncertainty of maize yield without nitrogen fertilization. Field Crop Res 260, 107985. https://doi.org/10.1016/j.fcr.2020.107985.

De Vries, W., Leip, A., Reinds, G.J., Kros, J., Lesschen, J.P., Bouwman, A., 2011. Comparison of land nitrogen budgets for European agriculture by various modeling approaches. Environ. Pollut. 159, 3254–3268. https://doi.org/10.1016/j.envpol.2011.03.038.

Del Grosso, S.J., Ogle, S.M., Parton, W.J., Breidt, F.J., 2010. Estimating uncertainty in N2O emissions from U.S. cropland soils. Global Biogeochem. Cycles 24, GB1009: 1–12. https://doi.org/10.1029/2009GB003544.

Dimkpa, C.O., Fugice, J., Singh, U., Lewis, T.D., 2020. Development of fertilizers for enhanced nitrogen use efficiency - Trends and perspectives. Sci. Total Environ. 731, 139113 https://doi.org/10.1016/j.scitotenv.2020.139113.

Dobermann, A., 2007. Nutrient use efficiency – measurement and management. In: Krauss, K.I., Heffer, P. (Eds.), Fertilizer Best Management Practice, General Principles, Strategy for their Adoption and Voluntary Initiatives vs. Regulations. IFA (International Fertilizer Association, Paris, pp. 1–28.

Dobermann, A., Cassman, K.G., 2005. Cereal area and nitrogen use efficiency are drivers of future nitrogen fertilizer consumption. Sci. China C Life Sci. 48, 745–758. https://doi.org/10.1007/BF03187115.

Fixen, P., Brentrup, F., Bruulsema, T., Garcia, F., Norton, R., Zingore, S., 2015. Nutrient/fertilizer use efficiency: measurement, current situation and trends. Managing water and fertilizer for sustainable agricultural intensification, 270. International Fertilizer Industry Association, International Water Management Institute, International Plant Nutrition Institute, International Potash Institute, pp. 1–30.

Gu, B., Ju, X., Chang, J., Ge, Y., Vitousek, P.M., 2015. Integrated reactive nitrogen budgets and future trends in China. Proc. National Acad. Sci., USA. https://doi.org/10.1073/pnas.1510211112.

Harris, I., Jones, P.D., Osborn, T.J., Lister, D.H., 2014. Updated high-resolution grids of monthly climatic observations – the CRU TS3. 10 Dataset. Int. J. Climatol. 34, 623–642. https://doi.org/10.1002/joc.3711.

He, W., Jiang, R., He, P., Yang, J., Zhou, W., Ma, J., Liu, Y., 2018. Estimating soil nitrogen balance at regional scale in China's croplands from 1984 to 2014. Agr. Syst. 167, 125–135. https://doi.org/10.1016/j.agsy.2018.09.002.

Helfenstein, A., Mulder, V.L., Heuvelink, G.B.M., Okx, J.P., 2022. Tier 4 maps of soil pH at 25 m resolution for the Netherlands. Geoderma 410, 115659. https://doi.org/10.1016/j.geoderma.2021.115659.

Hengl, T., Heuvelink, G.B.M., Kempen, B., Leenaars, J.G., Walsh, M.G., Shepherd, K.D., Sila, A., MacMillan, R.A., Mendes de Jesus, J., Tamene, L., Tondoh, J.E., 2015. Mapping soil properties of Africa at 250 m resolution: random forests significantly improve current predictions. PLoS One 10, e0125814. https://doi.org/10.1371/journal.pone.0125814.

Hengl, T., Mendes de Jesus, J., Heuvelink, G.B.M., Ruiperez Gonzalez, M., Kilibarda, M., Blagotic, A., Shangguan, W., Wright, M.N., Geng, X., Bauer-Marschallinger, B., Guevara, M.A., Vargas, R., MacMillan, R.A., Batjes, N.H., Leenaars, J.G.B., Ribeiro, E., Wheeler, I., Mantel, S., Kempen, B., 2017. SoilGrids250m: Global gridded soil information based on machine learning. PLoS One 12, e0169748. https://doi.org/10.1371/journal.pone.0169748.

Heuvelink, G.B.M., 1998a. In: Error Propagation in Environmental Modelling with GIS. CRC Press. https://doi.org/10.4324/9780203016114.

Heuvelink, G.B.M., 1998b. Uncertainty analysis in environmental modelling under a change of spatial scale. Nutr. Cycl. Agroecosyst. 50, 255–264. https://doi.org/10.1007/978-94-017-3021-1_24.

Heuvelink, G.B.M., Burrough, P.A., Stein, A., 1989. Propagation of errors in spatial modelling with GIS. Int. J. Geogr. Inform. Syst. 3, 303–322. https://doi.org/10.1080/02693798908941518.

Hounkpatin, K.O., Bossa, A.Y., Yira, Y., Igue, M.A., Sinsin, B.A., 2022. Assessment of the soil fertility status in Benin (West Africa) – Digital soil mapping using machine learning. Geoderma Reg. 28, e00444. https://doi.org/10.1016/j.geodrs.2021.e00444.

Huang, X., Song, Y., Li, M., Li, J., Huo, Q., Cai, X., Zhu, T., Hu, M., Zhang, H., 2012. A high-resolution ammonia emission inventory in China. Global Biogeochem. Cycles 26, GB1030: 1–14. https://doi.org/10.1029/2011GB004161.

Jiao, J., Li, J., Bai, Y., 2019. Uncertainty analysis in the life cycle assessment of cassava ethanol in China. J. Clean. Prod. 206, 438–451. https://doi.org/10.1016/j.jclepro.2018.09.199.

Kay, A., Davies, H., Bell, V., Jones, R., 2009. Comparison of uncertainty sources for climate change impacts: flood frequency in England. Clim. Change 92, 41–63. https://doi.org/10.1007/s10584-008-9471-4.

Knape, J., Valpine, P.D., 2016. Monte Carlo estimation of stage structured development from cohort data. Ecology 97, 992. https://doi.org/10.1890/15-0942.1.

Kros, J., Heuvelink, G.B.M., Reinds, G.J., Lesschen, J.P., Ioannidi, V., De Vries, W., 2012. Uncertainties in model predictions of nitrogen fluxes from agro-ecosystems in Europe. Biogeosciences 9, 4573–4588. https://doi.org/10.5194/bg-9-4573-2012.

Lalitha, M., Dharumarajan, S., Suputhra, A., Kalaiselvi, B., Hegde, R., Reddy, R., Prasad, C., Harindranath, C., Dwivedi, B., 2021. Spatial prediction of soil depth using environmental covariates by quantile regression forest model. Environ. Monit. Assess. 193, 1–10. https://doi.org/10.1007/s10661-021-09348-9.

Lassaletta, L., Billen, G., Grizzetti, B., Anglade, J., Garnier, J., 2014. 50 year trends in nitrogen use efficiency of world cropping systems the relationship between yield and nitrogen input to cropland. Environ. Res. Lett. 9, 105011 https://doi.org/10.1088/1748-9326/9/10/105011.

Lemaire, G., Ciampitti, I., 2020. Crop mass and N status as prerequisite covariables for unraveling nitrogen use efficiency across genotype-by-environment-by-management scenarios: a review. Plants 9, 1309. https://doi.org/10.3390/plants9101309.

Li, Y., Cui, S., Zhang, Z., Zhuang, K., Wang, Z., Zhang, Q., 2020. Determining effects of water and nitrogen input on maize (Zea mays) yield, water- and nitrogen-use efficiency: A global synthesis. Sci. Rep. 10, 9699. https://doi.org/10.1038/s41598-020-66613-6.

Liu, B., Zhao, X., Li, S., Zhang, X., Virk, A.L., Qi, J., Kan, Z., Wang, X., Ma, S., Zhang, H., 2020a. Meta-analysis of management-induced changes in nitrogen use efficiency of winter wheat in the North China Plain. J. Clean. Prod. 251, 119632 https://doi.org/10.1016/j.jclepro.2019.119632.

Liu, Y., Heuvelink, G.B.M., Bai, Z., He, P., Xu, X., Ma, J., Masiliūnas, D., 2020b. Space-time statistical analysis and modelling of nitrogen use efficiency indicators at provincial scale in China. Eur. J. Agron. 115, 126031 https://doi.org/10.1016/j.eja.2020.126032.

Liu, Y., Heuvelink, G.B.M., Bai, Z., He, P., Jiang, R., Huang, S., Xu, X., 2022. Statistical analysis of nitrogen use efficiency in Northeast China using multiple linear regression and random forest. J. Integr. Agric. 21, 3637–3657. https://doi.org/10.1016/j.jia.2022.08.054.

Liu, J., Li, Y., Huang, G., Zhuang, X., Fu, H., 2017. Assessment of uncertainty effects on crop planning and irrigation water supply using a Monte Carlo simulation based dual-interval stochastic programming method. J. Clean. Prod. 149, 945–967. https://doi.org/10.1016/j.jclepro.2017.02.100.

Lobell, D.B., 2007. The cost of uncertainty for nitrogen fertilizer management: A sensitivity analysis. Field Crop Res 100, 210–217. https://doi.org/10.1016/j.fcr.2006.07.007.

Lobell, D.B., Field, C.B., 2007. Global scale climate–crop yield relationships and the impacts of recent warming. Environ. Res. Lett. 2, 014002 https://doi.org/10.1088/1748-9326/2/1/014002.

Luo, Z., Lam, S.K., Fu, H., Hu, S., Chen, D., 2019. Temporal and spatial evolution of nitrous oxide emissions in China: Assessment, strategy and recommendation. J. Clean. Prod. 223, 360–367. https://doi.org/10.1016/j.jclepro.2019.03.134.

Meinshausen, N., 2006. Quantile regression forests. J. Mach. Learn. Res. 7, 983–999. https://doi.org/10.5555/1248547.1248582.

Miller, C.M.F., Waterhouse, H., Harter, T., Fadel, J.G., Meyer, D., 2020. Quantifying the uncertainty in nitrogen application and groundwater nitrate leaching in manure based cropping systems. Agr. Syst. 184, 102877 https://doi.org/10.1016/j.agsy.2020.102877.

Nigon, T.J., Yang, C., Paiao, G.D., Mulla, D.J., Fernández, F., 2020. Prediction of early season nitrogen uptake in maize using high-resolution aerial hyperspectral imagery. Remote Sens. (Basel) 12, 1234. https://doi.org/10.3390/rs12081234.

Nol, L., Heuvelink, G.B.M., Veldkamp, A., De Vries, W., Kros, J., 2010. Uncertainty propagation analysis of an N2O emission model at the plot and landscape scale. Geoderma 159, 9–23. https://doi.org/10.1016/j.geoderma.2010.06.009.

Poggio, L.M., de Sousa, L., Batjes, N.H., Heuvelink, G.B.M., Kempen, B., Riberio, E., Rossiter, D., 2020. SoilGrids 2.0: producing quality-assessed soil information for the globe. Soil Discuss. 1 https://doi.org/10.5194/soil-2020-65.

Porwollik, V., Müller, C., Elliott, J., Chryssanthacopoulos, J., Iizumi, T., Ray, D.K., Ruane, A.C., Arneth, A., Balkovič, J., Ciais, P., Deryng, D., Folberth, C., Izaurralde, R. C., Jones, C.D., Khabarov, N., Lawrence, P.J., Liu, W., Pugh, T.A.M., Reddy, A., Sakurai, G., Schmid, E., Wang, X., de Wit, A., Wu, X., 2017. Spatial and temporal uncertainty of crop yield aggregations. Eur. J. Agron. 88, 10–21. https://doi.org/10.1016/J.EJA.2016.08.006.

Quan, Z., Zhang, X., Fang, Y., Davidson, E.A., 2021. Different quantification approaches for nitrogen use efficiency lead to divergent estimates with varying advantages. Nature Food 2, 241–245. https://doi.org/10.1038/s43016-021-00263-3.

Ren, K.Y., Duan, Y.H., Minggang, X.U., Zhang, X.B., 2019. Effect of manure application on nitrogen use efficiency of crops in China: a meta-analysis. Sci. Agric. Sin. 52, 2983–2993. https://doi.org/10.3864/j.issn.0578-1752.2019.17.007 (in Chinese with English abstract).

Roberts, T., 2007. Right product, right rate, right time and right place… the foundation of best management practices for fertilizer. Fertilizer Best Management Practices 29, 1–8.

Robinson, R.L.M., Palczewska, A., Palczewski, J., Kidley, N., 2017. Comparison of the predictive performance and interpretability of random forest and linear models on benchmark data sets. J. Chem. Inform. Modeling 57, 1773–1792. https://doi.org/10.1021/acs.jcim.6b00753.

Shangguan, W., Dai, Y., Duan, Q., Liu, B., Yuan, H., 2014. A global soil data set for earth system modeling. J. Adv. Model. Earth Syst. 6, 249–263. https://doi.org/10.1002/2013MS000293.

Sonnemann, G.W., Schuhmacher, M., Castells, F., 2003. Uncertainty assessment by a Monte Carlo simulation in a life cycle inventory of electricity produced by a waste incinerator. J. Clean. Prod. 11, 279–292. https://doi.org/10.1016/S0959-6526(02)00028-8.

Stewart, W.M., Dibb, D.W., Johnston, A.E., Smyth, T.J., 2005. The contribution of commercial fertilizer nutrients to food production. Agron. J. 97, 1–6. https://doi.org/10.2134/agronj2005.0001.

Vaysse, K., Lagacherie, P., 2017. Using quantile regression forest to estimate uncertainty of digital soil mapping products. Geoderma 291, 55–64. https://doi.org/10.1016/j.geoderma.2016.12.017.

Venables, W.N., Ripley, B.D., 2002. In: Modern Applied Statistics with S. Springer, New York. https://doi.org/10.1007/978-0-387-21706-2.

Wang, E., Martre, P., Zhao, Z., Ewert, F., Maiorano, A., Rotter, R.P., Kimball, B.A., Ottman, M.J., Wall, G.W., White, J.W., Reynolds, M.P., Alderman, P.D., Aggarwal, P. K., Anothai, J., Basso, B., Biernath, C., Cammarano, D., Challinor, A.J., De Sanctis, G., Doltra, J., Dumont, B., Fereres, E., Garcia-Vila, M., Gayler, S., Hoogenboom, G., Hunt, L.A., Izaurralde, R.C., Jabloun, M., Jones, C.D., Kersebaum, K.C., Koehler, A.K., Liu, L., Muller, C., Naresh Kumar, S., Nendel, C., O'Leary, G., Olesen, J.E., Palosuo, T., Priesack, E., Eyshi Rezaei, E., Ripoche, D., Ruane, A.C., Semenov, M.A., Shcherbak, I., Stockle, C., Stratonovitch, P., Streck, T., Supit, I., Tao, F., Thorburn, P., Waha, K., Wallach, D., Wang, Z., Wolf, J., Zhu, Y., Asseng, S., 2017. The uncertainty of crop yield projections is reduced by improved temperature response functions. Nat. Plants 3, 17102. https://doi.org/10.1038/nplants.2017.125.

Wang, H., Zhou, J., 2014. Calculation of real fertilizer use efficiency and discussion on fertilization strategies. in Chinese Acta Pedol. Sin. 51, 216–225. https://doi.org/10.11766/trxb201312110588.

Xu, R., Tian, H., Pan, S., Prior, S.A., Feng, Y., Batchelor, W.D., Chen, J., Yang, J., 2019. Global ammonia emissions from synthetic nitrogen fertilizer applications in agricultural systems: Empirical and process-based estimates and uncertainty. Glob. Chang. Biol. 25, 314–326. https://doi.org/10.1111/gcb.14499.

Yang, F., Xu, X., Ma, J., He, P., Pampolino, M.F., Zhou, W., 2017. Experimental validation of a new approach for rice fertiliser recommendations across smallholder farms in China. Soil Res. 55, 579–589. https://doi.org/10.1071/SR16328.

Zhang, X., Davidson, E.A., Mauzerall, D.L., Searchinger, T.D., Dumas, P., Shen, Y., 2015. Managing nitrogen for sustainable development. Nature 528, 51–59. https://doi.org/10.1038/nature15743.

Zhang, X., Ren, C., Gu, B., Chen, D., 2021a. Uncertainty of nitrogen budget in China. Environ. Pollut. 286, 117216 https://doi.org/10.1016/j.envpol.2021.117216.

Zhang, X., Zou, T., Lassaletta, L., Mueller, N.D., Tubiello, F.N., Lisk, M.D., Lu, C., Conant, R.T., Dorich, C.D., Gerber, J., Tian, H., Bruulsema, T., Maaz, T.M., Nishina, K., Bodirsky, B.L., Popp, A., Bouwman, L., Beusen, A., Chang, J., Havlík, P., Leclère, D., Canadell, J.G., Jackson, R.B., Heffer, P., Wanner, N., Zhang, W., Davidson, E.A., 2021b. Quantification of global and national nitrogen budgets for crop production. Nature Food 2, 529–540. https://doi.org/10.1038/s43016-021-00318-5.

Zheng, J., Yin, S., Kang, D., Che, W., Zhong, L., 2012. Development and uncertainty analysis of a high-resolution NH_3 emissions inventory and its implications with precipitation over the Pearl River Delta region, China. Atmos. Chem. Phys. 12, 7041–7058. https://doi.org/10.5194/acp-12-7041-2012.